Supplementary Information

Photo- and pH Responsive Giant Vesicles: Harnessing the Properties of Surface-Active Ionic Liquids In designing Dual Responsive Catanionic Vesicles

Tapas Patel[a], Raviraj Pansuriya[a], Hemant Mittal[b], Sugam Kumar[b], Vinod K Aswal[b], Naved I Malek[a]*

[a]Ionic Liquids Research laboratory, Department of Chemistry, Sardar Vallabhbhai National Institute of Technology, Surat- 07, India

[b]DEWA R & D Centre, Dubai Electricity & Water Authority (DEWA), P.O.Box 564, Dubai, United Arab Emirates

[c]Solid State Physics Division, Bhabha Atomic Research Centre, Trombay, Mumbai-400085, India

Corresponding Author E-mail address: navedmalek@chem.svnit.ac.in

Small-Angle Neutron Scattering (SANS)

In a Small Angle Neutron Scattering (SANS) experiment, the typical measurement is the differential scattering cross section (dΣ/dΩ) per unit volume, which is a function of the wave vector transfer (Q). This can be articulated for monodispersed particles in a medium.

$$\frac{d\Sigma}{d\Omega} = nP(Q)S(Q) + B \tag{1}$$

In this context, 'n' represents the density of the particles. P(Q) is the intra-particle structure factor (which is the square of the form factor), and S(Q) is the inter-particle structure factor. P(Q) determines the specific size and shape of the scattering particle, while S(Q) establishes the spatial distribution of the particles, providing information about the interaction between particles. For a system that is dilute, S(Q) can be approximated as one. 'B' is a constant that signifies the incoherent background, primarily due to the presence of hydrogen atoms in the sample.

For prolate ellipsoidal particles, P(Q) can be expressed as

$$P(Q) = \frac{16\pi^2}{9}(\rho_p - \rho_s)^2(ab^2)^2 \int_0^1 [F(Q,\mu)]^2 d\mu \tag{2}$$

where the functions are given by

$$F(Q,\mu) = \frac{3(\sin x - x\cos x)}{x^3} \quad \text{and} \quad x = Q[a^2\mu^2 + b^2(1-\mu^2)]^{1/2} \tag{3}$$

where a and $b=c$ are, respectively semi-major and semi-minor axes of prolate ellipsoid ($a>b=c$). The variable x is the cosine of the angle between the directions of a and Q.

The following expression provides $P(Q)$ for a spherical core-shell structure,

$$P(Q) = \frac{16\pi^2}{9}[(R+\mathrm{dR})^3(\rho_{\mathrm{shell}}-\rho_s)\frac{\mathrm{sinQ}(R+\mathrm{dR})-Q(R+\mathrm{dR})\mathrm{cosQ}(R+\mathrm{dR})}{Q^3(R+\mathrm{dR})^3}$$
$$\frac{\mathrm{sinQR}-\mathrm{QRcosQR}}{Q^3R^3}]^2$$

Where R is core radius and dR is shell thickness. r_{core} and r_{shell} represents the scattering length densities of the core and shell, respectively.

Throughout the data analysis corrections were made for instrumental smearing. The calculated scattering profiles were smeared by the appropriate resolution function to compare with the measured data. The parameters in the analysis were optimized by means of a nonlinear least-square fitting program.[1]

Turbidity study of aggregates

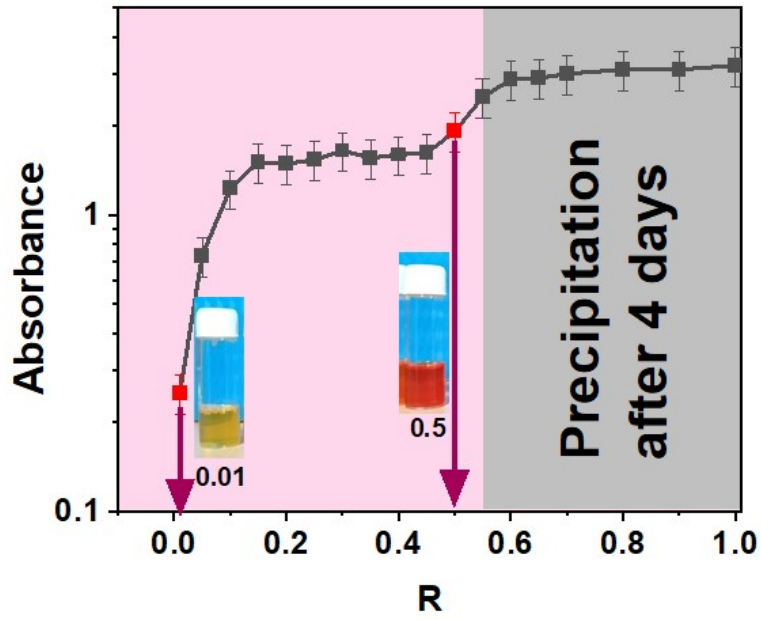

Figure S1: Turbidity study: absorption value of [C_8EMorph][MO]/[Ch][Ol] systems at different concentrations of [C_8EMorph][MO].

Absorption of SAILs at the solution/air interface

The graph of surface tension of the aqueous [C_8EMorph][MO] solution as a function of concentration is given in **Figure S2(a)**. The previously reported SAIL named [C_8EMorph][Br] is having cmc of 63.35 mM.[2] Herein, we have replaced bromine anion with bulky anion MO, to aim the impact of the head group on the surface active properties. The decreased cmc of [C_8EMorph][MO] after replacing the MO is 6.83 mM, which is much lower (~9.3 times) than the [C_8EMorph][Br]. The cmc obtained from the surface tension graph (**Figure S2(b)**) for [Ch][Ol] is well agreed with the literature.[3] Further, for the aqueous solution of [C_8EMorph][MO] and [Ch][Ol], we have measured the surface active parameters. A significant change in the value of surface tension at cmc (γ_{CMC}) was observed for both SAILs (**Table S1**). Similar findings were noted for the surface pressure at the cmc (π cmc). These were based on the maximum surface excess concentration values($\mathbf{\Gamma}_{max}$), [C_8EMorph][MO] and [Ch][Ol] are available in larger amount at the air/solution interface. Additionally, the obtained values for A_{min} (the minimum area occupied by an amphiphilic molecule at the solution/air interface) were nearly identical.

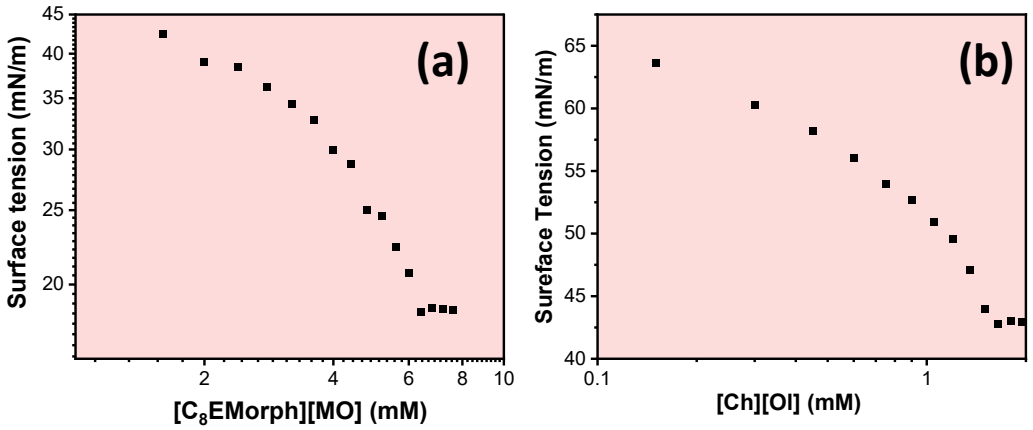

Figure S2: Surface tension curve of concentration of **(a)** [C_8EMorph][MO] and **(b)** [Ch][Ol] vs Surface tension at 25 ^{0}C.

Table S1: Computed parameters from surface tension data for the [C_8EMorph][MO] and [Ch][Ol] at 25 ^{0}C.

SAILs	cmc (mM)	γ_{cmc} (mN/m)	Π_{cmc} (mN/m)	Γ_{max} x 10^6 (mol/m^2)	A_{min} (Å^2)	Reference
[C_8EMorph][Br]	63.35	25.0	47.20	1.42	117	[2]
[C_8EMorph][MO]	6.83	42.8	28.7	3.11	53	This work
[Ch][Ol]	1.71	25.4	46.1	3.31	50	This work

The uncertainties in the calculated parameters are: γ_{cmc} = ±0.1 mN/m; π_{cmc} = ±0.1 mN/m; Γ_{max} = ±0.2x 10^{-6} mol/m^2; A_{min} = 0.5 Å^2

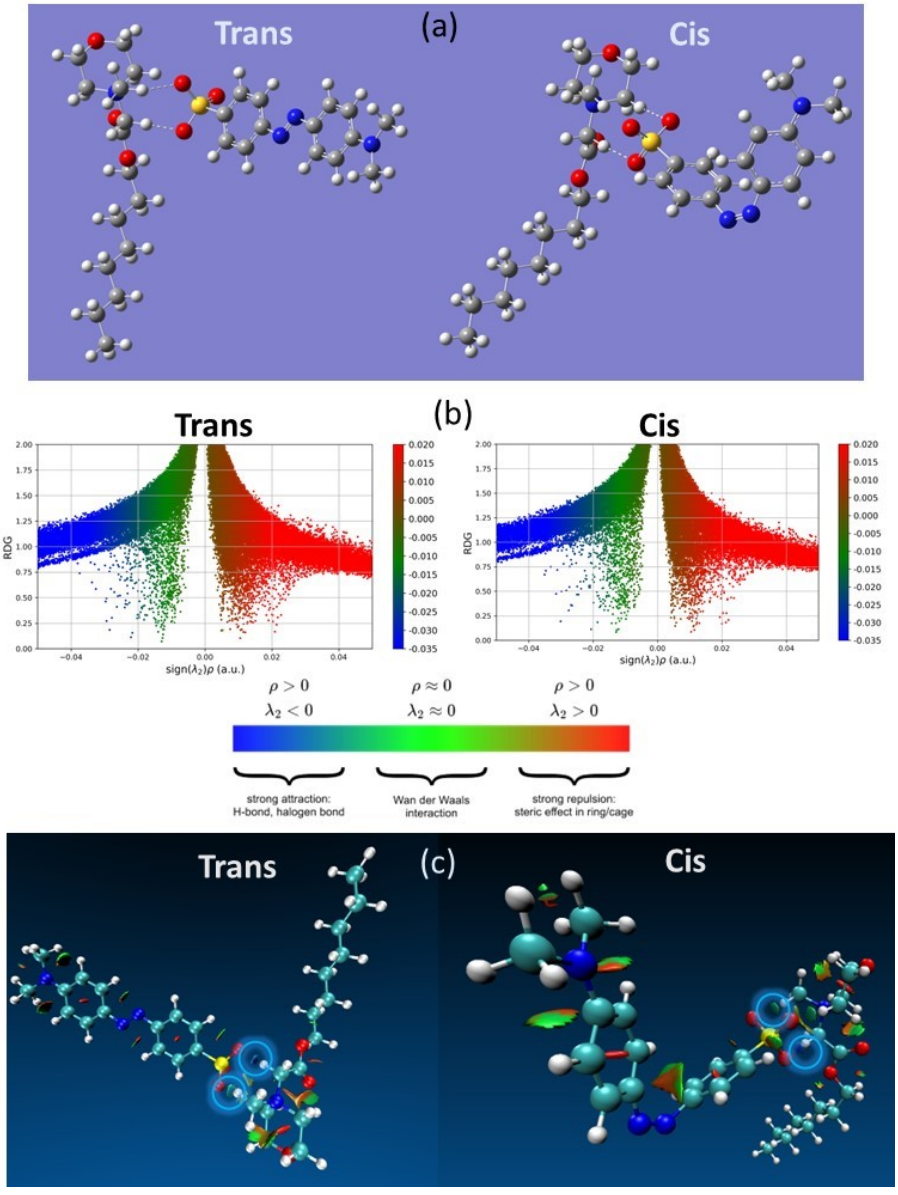

Figure S3: (a) Ground state optimized structures of E-Z [C_8EMorph][MO], (b) RDG scatter graphs of both E-Z [C_8EMorph][MO], and (c) NCI plots of E-Z [C_8EMorph][MO] (VMD)

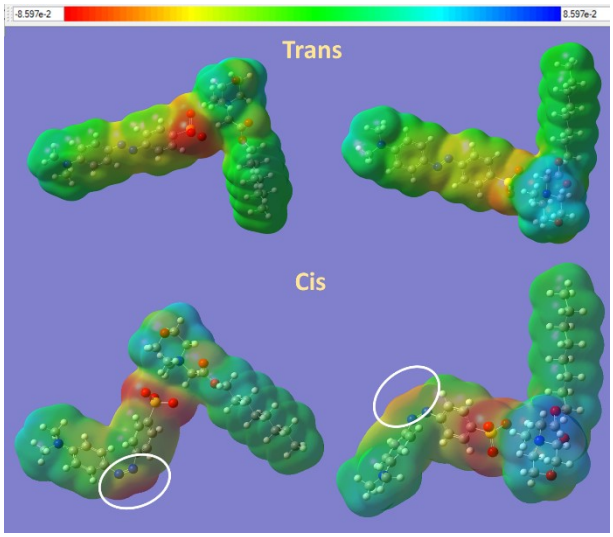

Figure S4: Electrostatic potential plots of both trans and cis isomers of [C_8EMorph][MO] from two different angles.

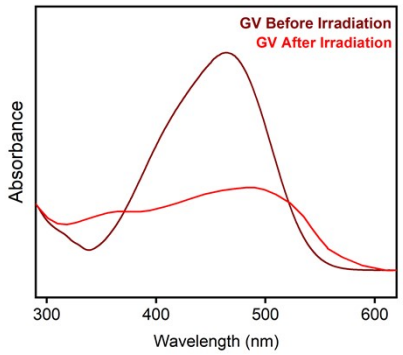

Figure S5: Absorption spectra of GV before and after UV irradiation.

When GV is exposed to light irradiation, the trans isomers of [C_8EMorph][MO] undergo a conversion to their cis isomeric form. This isomerization within GV is evidenced by the changes observed in the absorption spectra (Figure S5). Prior to irradiation, GV exhibited an absorbance peak at 0.83. Following 30 minutes of light exposure, this absorbance value decreased to 0.32. Moreover, the trans [C_8EMorph][MO] exhibited a peak absorbance at 0.83, whereas the cis [C_8EMorph][MO] demonstrated a reduced absorbance at 0.27.

$$Degree\ of\ isomerization = \left(\frac{A_{GV} - A^{*}_{GV}}{A_{trans} - A^{*}_{cis}}\right) \times 100\ \%$$

Where, A_{GV}: Absorbance of GV before light irradiation.

A_{GV}^{*}: Absorbance of GV after light irradiation.

A_{trans}: Absorbance of trans IL.

A_{cis}^{*}: Absorbance of cis IL.

Utilizing these absorbance values, the degree of isomerization of GV after the irradiation period was calculated to be 91%.

Zeta potential of GV system as a function of pH.

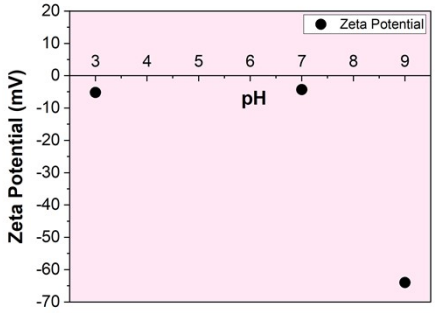

Figure S6: Zeta potential of GV system as a function of pH

Effect of dilution and time stability study

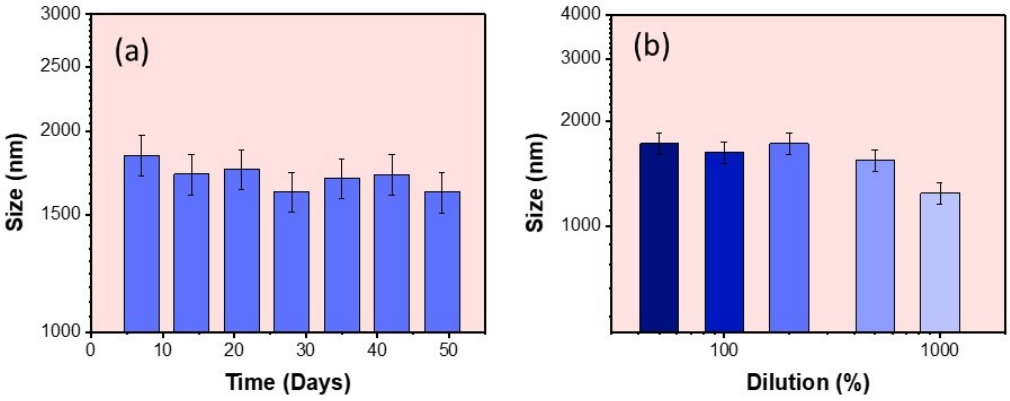

Figure S7: Stability of GV as a function of (a) time vs size and (b) dilution vs size

References

1 D. I. Svergun and M. H. J. Koch, *Reports on Progress in Physics*, 2003, **66**, 1735–1782.

2 S. M. Rajput, M. Kuddushi, A. Shah, D. Ray, V. K. Aswal, S. K. Kailasa and N. I. Malek, *Surfaces and Interfaces*, 2020, **20**, 100596.

3 M. K. Ali, R. M. Moshikur, R. Wakabayashi, Y. Tahara, M. Moniruzzaman, N. Kamiya and M. Goto, *J Colloid Interface Sci*, 2019, **551**, 72–80.